

Highly fluorinated metal complexes as dual ^{19}F and PARACEST imaging agents

Meng Yu, Bailey S. Bouley, Da Xie, Emily L. Que*

Department of Chemistry, University of Texas at Austin, Austin, TX 78712, United States

Materials and Methods	S2
Synthetic Methods	S3
Scheme S1. Synthesis of fluorine tag 11	S3
Scheme S2. Synthesis of ligand L	S4
Figure S1. ^{19}F NMR spectra of 1 mM FeL , CoL and NiL	S7
Figure S2. IR spectra of L , FeL , CoL and NiL	S8
Figure S3. Measured effect magnetic moments of FeL , CoL , and NiL at different pH	S8
Figure S4. ^{19}F MR images of FeL , CoL , NiL , and L at different concentrations	S9
Figure S5. ^1H NMR spectra of FeL in HEPES buffer solutions of H_2O and D_2O	S9
Figure S6. ^1H NMR spectra of CoL in HEPES buffer solutions of H_2O and D_2O	S10
Figure S7. ^1H NMR spectra of NiL in HEPES buffer solutions of H_2O and D_2O	S10
Figure S8. CEST spectra for 10.5 mM FeL in HEPES at pH 6.50-8.06	S11
Figure S9. CEST spectra 8.5 mM FeL in HEPES at pH 7.32 with power level (B_1) from 14.0 μT to 25.0 μT	S11
Figure S10. Measurement of proton exchange rates (k_{ex}) for FeL using Omega plot	S12
Figure S11. CEST spectra for 10.9 mM CoL in HEPES at pH 6.49-8.01.	S13
Figure S12. CEST intensity at 58 ppm and 52 ppm for 10.9 mM of CoL at pH 6.49-8.01	S13
Figure S13. Omega plots of CoL at 58 and 52 ppm for 10.0 mM of CoL in HEPES at pH 6.84–8.05	S14
Figure S14. Calculated k_{ex} values for CoL using Omega plot at different pH	S15
Figure S15. CEST spectra of NiL in HEPES buffered at pH 6.79-7.97.	S16
Figure S16. Measurement of proton exchange rates (k_{ex}) for NiL using Omega plot	S17
Figure S17. CEST percentages of FeL with variable concentrations at pH 7.4,	S18
Figure S18. High resolution mass spectrum of FeL	S18
Figure S19. High resolution mass spectrum of CoL	S19
Figure S20. High resolution mass spectrum of NiL .	S19
Figure S21. ^1H NMR spectrum of L in CD_3OD	S20
Figure S22. ^{19}F NMR spectrum of L in CD_3OD	S21
Figure S23. ^{13}C NMR spectrum of L in CD_3OD	S22
References	S22

Materials and Methods

Materials

Except where stated otherwise, all chemicals were purchased from Sigma-Aldrich and Fisher Scientific and used as received. 1,4,7,10-tetraazacyclododecane was purchased from Strem Chemicals. Deuterated solvents were purchased from Cambridge Isotope Laboratories. **2**¹, **8**², and **DO3AMCOOH**³ were synthesized according to modified literature procedures.

Instrumentation

All ¹H, ¹³C and ¹⁹F NMR spectra were recorded on a 400 MHz Agilent NMR spectrometer; all reported resonances were referenced to internal standards. ¹⁹F NMR peaks were referenced versus 5-fluorocytosine. T₁ relaxation time was determined using the inversion-recovery method and T₂ relaxation time was measured using the Carr-Purcell-Meiboom-Gill (CPMG) pulse sequence. Walk-up LC-MS and high-resolution Electrospray Ionization (ESI) mass spectral analyses were performed by the Mass Spectrometry Facility of the Department of Chemistry at UT Austin. Electrode-based pH measurements were carried out using a Thermo Scientific Orion 9110DJWP double junction pH electrode connected to a Sartorius PB-11 pH meter. Solid state infrared spectra were recorded on a Bruker Alpha spectrometer equipped with a diamond ATR crystal. UV/vis spectra were recorded on an Agilent Cary 6 UV/vis spectrometer. Magnetic resonance images were collected on a Bruker BioSpin (Karlsruhe, Germany) Pharmascan 70/16 magnet with a BioSpec two-channel console and BGA-9s gradient coil in the Imaging Research Center at UT Austin.

Determination of magnetic moment.

The effective magnetic moment was determined based on Evans' method.⁴ A solution of ~5 mM metal complex in 50 mM HEPES buffer and 100 mM at specific pH, containing 5% tert-butanol by volume was placed in an NMR coaxial tube with 5% tert-butanol (v/v) in D₂O as reference. The concentration of metal complex in stock solution was predetermined by ¹⁹F NMR using 5-fluorocytosine as an internal standard. The effective magnetic moment (μ_{eff}) was calculated at 298 K (T) by using the equations given below. Δf stands for the proton chemical shift of *tert*-butanol in frequency (Hz) between the reference and paramagnetic sample, the spectrometer frequency (f) in Hz, the mass of the substance per mL of the solution (m), and $\chi_{\text{M}}^{\text{dia}}$ is the diamagnetic contribution to the molar susceptibility (cm³ mol⁻¹). Diamagnetic corrections were carried out based on the empirical formula of the compound using Pascal's constants.⁵ The molar susceptibility (χ_{m}) is the product of χ_{g} times the molecular weight of metal complex.

$$\chi_{\text{g}} = (-3\Delta f)/(4\pi f m) - \chi_{\text{M}}^{\text{dia}} \text{ eq. (1)}$$

$$\mu_{\text{eff}} = 2.84 (\chi_{\text{m}} T)^{1/2} \text{ eq. (2)}$$

Air and aqueous stability of **FeL**, **CoL**, and **NiL**

1 mM aerated buffer solution (50 mM HEPES, 0.1 M NaCl, pH 7.4) of **FeL**, **CoL**, or **NiL** was prepared. The solution was exposed to atmosphere and the ¹⁹F NMR spectra (referenced to 5-fluorocytosine) were acquired routinely every 24 h over one week and no noticeable change was observed.

¹⁹F MRI Experiments

The magnetic resonance imaging experiments were performed on a Bruker BioSpin (Karlsruhe, Germany) Pharmascan 70/16 magnet with a BioSpec two-channel console and BGA-9s gradient coil. The RF coil was a quadrature single resonance tunable T/R coil (Doty Scientific, Inc., Columbia, South Carolina, USA) with a resonant frequency of 282.2 MHz to correspond to ¹⁹F at 7.0 T. Each element of the RF coil was tuned and matched with the samples loaded using a Morris frequency sweeper (Morris

Instruments, Inc. Ottawa, Ontario, Canada) while the complementary element was terminated with the receive chain of the instrument. All prescan adjustments and imaging was performed using product sequences and methods in ParaVision 6.0.1 (Bruker, vide supra).

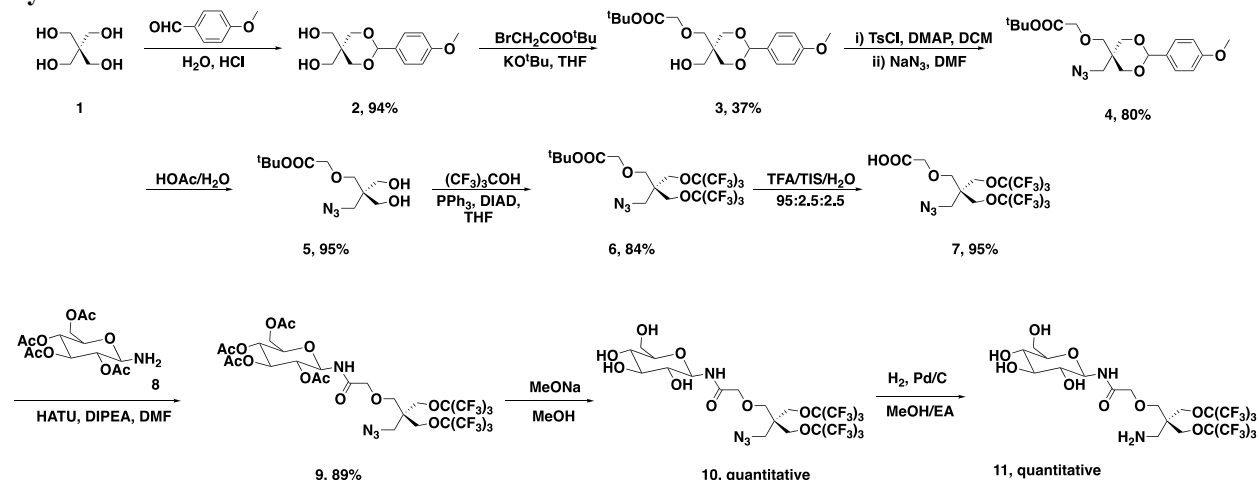
Solutions were imaged while contained in standard 600 μL Eppendorf tubes mounted in a 3 \times 3 grid by a custom holder produced on a Form 2 3D printer (FormLabs, Inc., Somerville, Massachusetts, USA). For limit of detection study, complexes were dissolved in 500 μL of 50 mM pH 7.4 HEPES buffer (0.1 M NaCl) at different concentrations with optimized RARE (Rapid Acquisition with Relaxation Enhancement) sequence parameters. RARE sequence parameters for **FeL**, **CoL** and **NiL**: TE (Echo Time) = 7.50 ms, TR (Repetition Time) = 100 ms, NA (Number of Averages) = 1250, FA (Flip Angle) = 90°, rare factor = 8, BW (Bandwidth) = 7.5 kHz, matrix size = 64 x 64, FOV (Field of View) = 40 x 40 mm, ST (Slice Thickness) = 50 mm, scan time = 12.5 min; RARE sequence parameters for **L**: TE = 14.99 ms, TR = 1500 ms, NA = 164, FA = 90°, rare factor = 16, BW = 7.5 kHz, matrix size = 64 x 64, FOV = 40 x 40 mm, ST = 50 mm, scan time = 12.5 min.

CEST Experiments

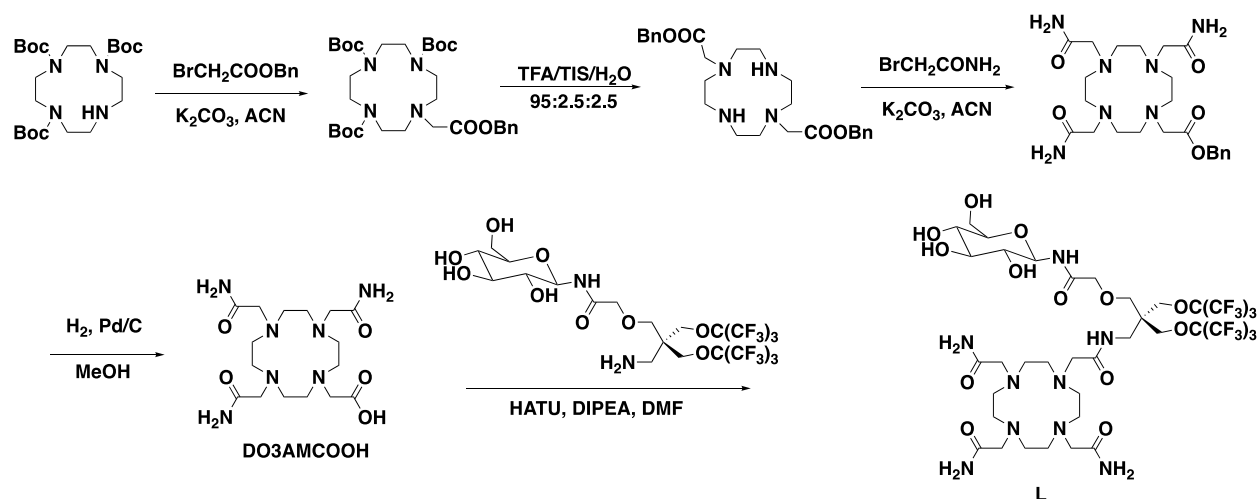
All CEST experiments were carried out at 23 °C on a Varian 400 MHz (9.4T) spectrometer. In specific, 5–20 mM complexes in aqueous buffer solutions containing 50 mM HEPES and 100 mM NaCl at different pH values (measured with a pH electrode before ^1H NMR and CEST data collection) were measured. Z-spectra (CEST spectra) were obtained according to the following protocol: ^1H NMR spectra were acquired from –45 to 95 ppm at 1 ppm increment using a presaturation pulse applied for 4 s at a power level (B_1) of 25 μT . An inner coaxial capillary tube containing D_2O was used to lock the samples. The normalized integrations of the H_2O signal from the obtained spectra were plotted against frequency offset to generate a Z-spectrum, where direct saturation of the H_2O signal was set to 0 ppm. CEST intensities are reported as %CEST = $[(1 - M_z/M_0) \times 100\%]$ (M_z and M_0 are the magnetization on-resonance and off-resonance values, respectively).

Exchange rate constants (k_{ex}) were calculated Omega plot, where the X-intercept ($-1/k_{\text{ex}}^2$) was obtained from a plot of $M_z/(M_0 - M_z)$ against $1/\omega_1^2$ (ω_1 in rad s^{-1}). ^1H NMR spectra were acquired at various presaturation power levels ranging from 14.0 to 25.0 μT applied for 4 s at 23 °C. The B_1 values were calculated based on the calibrated 90° pulse on a linear amplifier.

Synthetic Methods



Scheme S1. Synthesis of fluorine tag **11**.



Scheme S2. Synthesis of ligand L.

3

2 (20.0 g, 78.6 mmol) was dissolved in 80 mL dry DMF and KO^tBu (20% in THF solution, 47.5 mL, 77 mmol) was added and stir for 15 min. The solution was cooled with an ice bath and BrCH₂COO^tBu (30.7 g, 157.4 mmol) was added dropwise. The mixture was then heated to 65 °C for 48 h and solvent was removed by evaporation. 200 mL NaHCO₃ (sat.) was added and extracted with DCM. The organic layers were combined and purified by column (Hexanes/EA 6:1 to 3:2) to obtain 9.6 g product as a colorless oil. ¹H NMR (400 MHz, Chloroform-*d*) δ 7.45 – 7.37 (m, 2H), 6.92 – 6.86 (m, 2H), 5.37 (s, 1H), 4.09 (d, *J* = 7.1 Hz, 1.5 H), 4.02 (s, 0.5 H), 3.93 (d, *J* = 6.4 Hz, 2H), 3.80 (s, 3H), 3.75 – 3.65 (m, 2H), 3.49 – 3.41 (m, 1H), 3.30 (s, 2H), 1.49 (d, *J* = 2.4 Hz, 9H). Note that there are isomers present in the system resulting in non-integers of peak integration. ¹³C NMR (101 MHz, Chloroform-*d*) δ 170.62, 160.00, 127.43, 127.30, 113.63, 101.92, 82.70, 71.84, 70.78, 70.49, 70.10, 67.86, 63.85, 62.01, 55.31, 39.25, 39.07, 28.09.

4

3 (9.2 g, 24.8 mmol) and 4-dimethylaminopyridine (DMAP) (4.6 g, 37.2 mmol) were dissolved in 100 mL dry DCM and the mixture was cooled down to 0 °C using an ice bath. *p*-Toluenesulfonyl chloride (7.1 g, 37.2 mmol) was added in one portion and the solution was stirred under R.T. for 16 h. The solution was then washed with NaHCO₃ (sat., 50 mL x 2) and brine (50 mL x 3) and purified by column (ethyl acetate/hexanes 1:10 to 1:4). The tosylated product (8.5 g, 16.3 mmol) was dissolved in 80 mL dry DMF and NaN₃ (1.5 g, 23.1 mmol) was added. The solution was heated to 120 °C and reacted for 48 h. DMF was then removed and 100 mL water was added. The solution was extracted with DCM and the crude was purified by column (hexanes/EA 20:3) to yield 6.6 g product as a colorless oil. ¹H NMR (400 MHz, Chloroform-*d*) δ 7.44 – 7.36 (m, 2H), 6.89 (m, 2H), 5.38 (d, *J* = 6.5 Hz, 1H), 4.16 – 4.00 (m, 3H), 3.97 – 3.72 (m, 8H), 3.33 (d, *J* = 14.6 Hz, 2H), 1.48 (d, *J* = 3.3 Hz, 9H). ¹³C NMR (101 MHz, Chloroform-*d*) δ 169.47, 169.30, 160.07, 160.04, 130.39, 127.34, 113.67, 113.62, 101.94, 101.72, 81.89, 81.69, 70.96, 70.33, 70.08, 69.99, 69.19, 68.92, 55.32, 52.42, 51.45, 38.62, 38.42, 28.14, 28.10.

5

4 (4.5 g, 11.4 mmol) was dissolved in AcOH/H₂O (50 mL, 4:1) and heated at 50 °C for 3 h. The solvent was removed and 50 mL water was added. The solution was extracted with EtOAc and purified by column (hexanes/EA 10:1 to 1:1) to get 3.0 g product as a colorless oil. ¹H NMR (400 MHz, Chloroform-*d*) δ 3.95 (s, 2H), 3.68 – 3.57 (m, 4H), 3.50 (s, 2H), 3.37 (s, 2H), 1.47 (s, 9H). ¹³C NMR (101 MHz, Chloroform-*d*) δ 171.12, 82.89, 70.25, 67.73, 63.33, 51.61, 45.48, 28.06.

6

PPh₃ (4.4 g, 21.8 mmol) was dissolved in 50 mL dry THF. The solution was cooled down to 0 °C using an ice bath and diisopropyl azodicarboxylate (DIAD) (5.7 g, 21.8 mmol) was added dropwise to form a white precipitate. The suspension was stirred under R.T. for 0.5 h and **5** (2.0 g, 7.3 mmol) was introduced to stir for another 10 min. Finally, (F₃C)₃COH (5.1 g, 21.8 mmol) was added and mixture was stirred under R.T. for 2 days. Solvent was removed and the crude was purified by silica gel chromatography (DCM/Hexanes 1:20 to 1:15) to yield 4.34 g product as a colorless oil. ¹H NMR (499 MHz, Chloroform-*d*) δ 4.06 (s, 4H), 3.92 (s, 2H), 3.51 (d, *J* = 7.1 Hz, 4H), 1.47 (s, 9H). ¹⁹F NMR (470 MHz, CDCl₃) δ -70.53. ¹³C NMR (126 MHz, CDCl₃) δ 167.80, 122.73, 122.70, 122.67, 120.37, 118.04, 118.01, 115.73, 115.69, 115.65, 80.88, 68.07, 67.13, 65.98, 48.88, 44.53, 26.97.

7

6 (1.2 g, 1.7 mmol) was dissolved in 10 mL TFA/triisopropylsilane/H₂O (95/2.5/2.5, v/v/v) and stirred at R.T. for 16 h. Solvent was then removed and the crude was purified by silica gel chromatography (DCM/MeOH, 8:1, containing 0.5% AcOH) to yield 1.1 g product as a white solid. ¹H NMR (400 MHz, Chloroform-*d*) δ 4.12 (s, 2H), 4.05 (s, 4H), 3.52 (d, *J* = 14.6 Hz, 4H). ¹⁹F NMR (376 MHz, Chloroform-*d*) δ -70.37.

9

Compound **7** (356 mg, 0.543 mmol) and hexafluorophosphate azabenzotriazole tetramethyl uranium (HATU) (292 mg, 0.768 mmol) were combined and dissolved with 4 mL anhydrous DMF. N,N-diisopropylethylamine (DIPEA) (223 μL, 1.28 mmol) was added and the solution was stirred on ice bath for 30 min. 2-(acetoxymethyl)-6-aminotetrahydro-2*H*-pyran-3,4,5-triyl triacetate **8** (356 mg, 1.02 mmol) predissolved in 2 mL anhydrous DMF was then introduced and the mixture was allowed to warm up to room temperature and stir for 16 h. DMF was removed under vacuum and the crude was subjected to reverse phase chromatography using H₂O/MeCN (0.1% HCOOH) as eluent. Fractions containing product were combined and lyophilized to obtain 470 mg product as a fluffy light yellow powder (88% yield). ¹H NMR (400 MHz, Chloroform-*d*) δ 7.34 (d, *J* = 9.0 Hz, 1H), 5.34 (t, *J* = 9.6 Hz, 1H), 5.20 (t, *J* = 9.2 Hz, 1H), 5.09 (dd, *J* = 10.1, 9.2 Hz, 1H), 4.89 (t, *J* = 9.6 Hz, 1H), 4.31 (dd, *J* = 12.5, 4.2 Hz, 1H), 4.17 – 3.99 (m, 5H), 3.96 (s, 2H), 3.85 (m, 1H), 3.67 – 3.50 (m, 2H), 3.45 (m, 2H), 2.58 – 1.72 (m, 12H); ¹⁹F NMR (376 MHz, Chloroform-*d*) δ -70.34 (d, *J* = 10.3 Hz); ¹³C NMR (101 MHz, Chloroform-*d*) δ 171.05, 170.60, 169.85, 169.56, 169.14, 121.52, 118.61, 77.78, 73.49, 72.35, 70.55, 70.37, 68.09, 67.92, 66.19, 61.50, 49.20, 45.48, 20.60, 20.58, 20.50.

10

Compound **9** (470 mg, 0.478 mmol) was dissolved in 3 mL anhydrous MeOH. 177 μL MeONa (5.4 M in MeOH) was then added. The solution was stirred under N₂ for 16 h and 5 mL distilled water was added. pH of the solution was adjusted to 5 with acetic acid followed by evaporation of MeOH. The remaining aqueous solution was extracted with EtOAc (5 x 30 mL) and dried over Na₂SO₄. Solvent was removed under vacuum to obtain product as a colorless oil (360 mg, 92%). ¹H NMR (400 MHz, Acetonitrile-*d*₃) δ 4.95 (t, *J* = 9.2 Hz, 1H), 4.18 – 4.07 (m, 4H), 4.02 – 3.93 (m, 2H), 3.74 (m, 1H), 3.63 – 3.48 (m, 5H), 3.45 – 3.19 (m, 4H); ¹⁹F NMR (376 MHz, Acetonitrile-*d*₃) δ -70.95; ¹³C NMR (101 MHz, Acetonitrile-*d*₃) δ 169.47, 121.65, 118.74, 78.97, 77.85, 77.38, 72.74, 70.40, 67.91, 66.86, 61.72, 49.41, 45.42.

11

Compound **10** (360 mg, 0.441 mmol) and Pd/C (100 mg) were suspended in 15 mL (EtOAc/MeOH, 3/1, v/v). The suspension was stirred under H₂ for 16 h and filtered through celite. The solvent was removed to yield 350 mg of product **11** as a colorless amorphous solid (quantitative yield). ¹H NMR (400 MHz, Methanol-*d*₄) δ 4.97 (s, 1H), 4.35 – 3.95 (m, 6H), 3.83 (m, 1H), 3.74 – 3.20 (m, 7H), 2.93 (s, 2H). ¹⁹F NMR (376 MHz, Methanol-*d*₄) δ -71.63; ¹³C NMR (101 MHz, Methanol-*d*₄) δ 178.90, 172.17, 124.53, 121.63, 118.72, 115.81, 79.39, 78.30, 77.37, 72.37, 69.88, 69.01, 68.14, 67.28, 61.12, 44.67, 40.21, 22.69.

Ligand (L)

DO3AMCOOH (150 mg, 0.374 mmol) and HATU (140 mg, 0.367 mmol) were dissolved in 3 mL anhydrous DMF. DIPEA (108 μ L, 0.621 mmol) was added and the mixture was stirred under N₂ at 0 °C for 20 min. Then compound **11** (245 mg, 0.310 mmol) predissolved in 3 mL dry DMF was introduced. The solution was warmed to room temperature and stirred for 16 h. DMF was then removed under vacuum and the crude was purified by reverse phase chromatography using H₂O/MeCN (0.1% HCOOH) as eluent. Product came out at 60% MeCN and fractions were combined and lyophilized to yield ~200 mg product as a white powder (55%). ¹H NMR (400 MHz, Methanol-*d*₄) δ 5.00 (d, *J* = 9.1 Hz, 1H), 4.24 – 3.96 (m, 6H), 3.84 (dd, *J* = 11.9, 2.2 Hz, 1H), 3.68-2.86 (m, 33H). ¹⁹F NMR (376 MHz, Methanol-*d*₄) δ -71.47; ¹³C NMR (101 MHz, Methanol-*d*₄) δ 168.87, 123.70, 121.38, 119.05, 116.73, 79.36, 78.43, 77.39, 72.56, 70.05, 69.27, 69.17, 67.95, 61.27, 56.52 (br), 51.87 (br), 45.35, 38.16.

FeL

L (32 mg, 0.0267 mmol) was dissolved in 5 mL degassed Milli-Q water and Fe(BF₄)₂•6H₂O (9.5 mg, 0.0281 mmol) was added. The solution was heated to 50 °C and stirred under N₂ for 48 h. The reaction was monitored using ¹⁹F NMR until no free ligand peak can be observed. The crude was purified by reverse phase chromatography using 50 mM ammonium acetate buffer (pH~6.5) and MeCN (contain 5% ammonium acetate buffer) as eluent (product came out at 50% MeCN) to yield about 25 mg white powder as the product. High-resolution mass spectrum (HRMS) (ESI⁺): Calcd for M²⁺ (C₃₇H₅₃F₁₈N₉O₁₃Fe) 614.6426, found 614.6407.

CoL

L (33 mg, 0.0281 mmol) was dissolved in 5 mL Milli-Q water (degassed) and Co(BF₄)₂•6H₂O (11.5 mg, 0.0338 mmol) was added. The solution was heated to 50 °C and stirred for 48 h. The reaction was monitored using ¹⁹F NMR until no free ligand peak can be observed. The crude was purified by reverse phase chromatography using 50 mM ammonium acetate buffer (pH~6.5) and MeCN (contain 5% ammonium acetate buffer) as eluent (product came out at 50% MeCN) to yield about 32 mg pink fluffy powder as the product. HRMS (ESI⁺): Calcd for M²⁺ (C₃₇H₅₃F₁₈N₉O₁₃Co) 616.1398, found 616.1412.

NiL

L (32 mg, 0.0267 mmol) was dissolved in 5 mL Milli-Q water and Ni(BF₄)₂•6H₂O (10 mg, 0.0294 mmol) was added. The solution was heated to 80 °C and stirred for 48 h. The reaction was monitored using ¹⁹F NMR until no free ligand peak can be observed. The crude was purified by reverse phase chromatography using 50 mM ammonium acetate buffer (pH~6.5) and MeCN (contain 5% ammonium acetate buffer) as eluent (product came out at 50% MeCN) to yield about 30 mg light purple solid as the product. HRMS (ESI⁺): Calcd for M²⁺ (C₃₇H₅₃F₁₈N₉O₁₃Ni) 615.6409, found 615.6421.

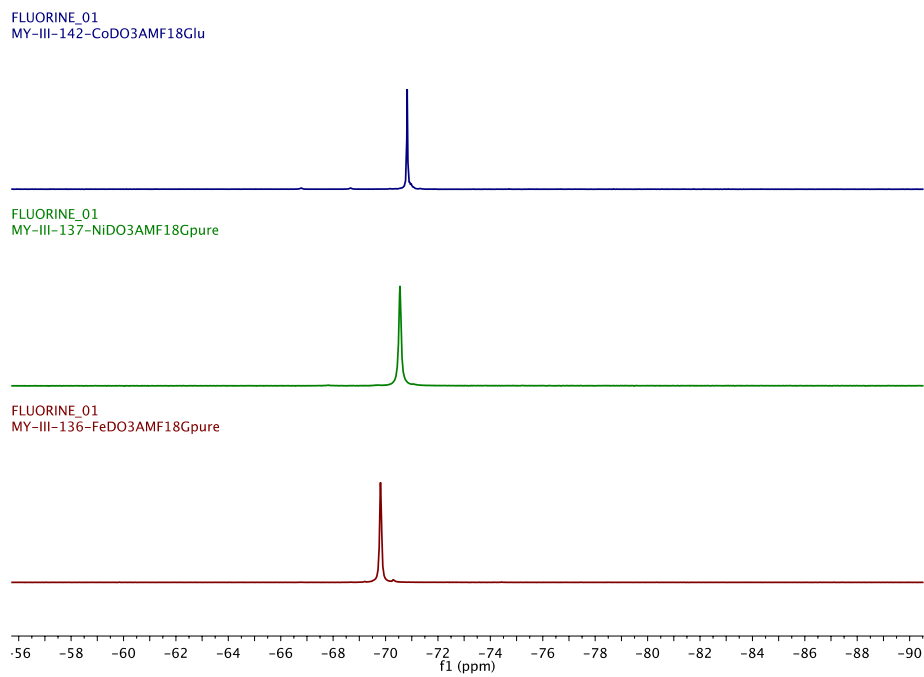


Figure S1. ^{19}F NMR spectra of 1 mM FeL, CoL, and NiL in 50 mM HEPES buffer (0.1 M NaCl, pH = 7.4).

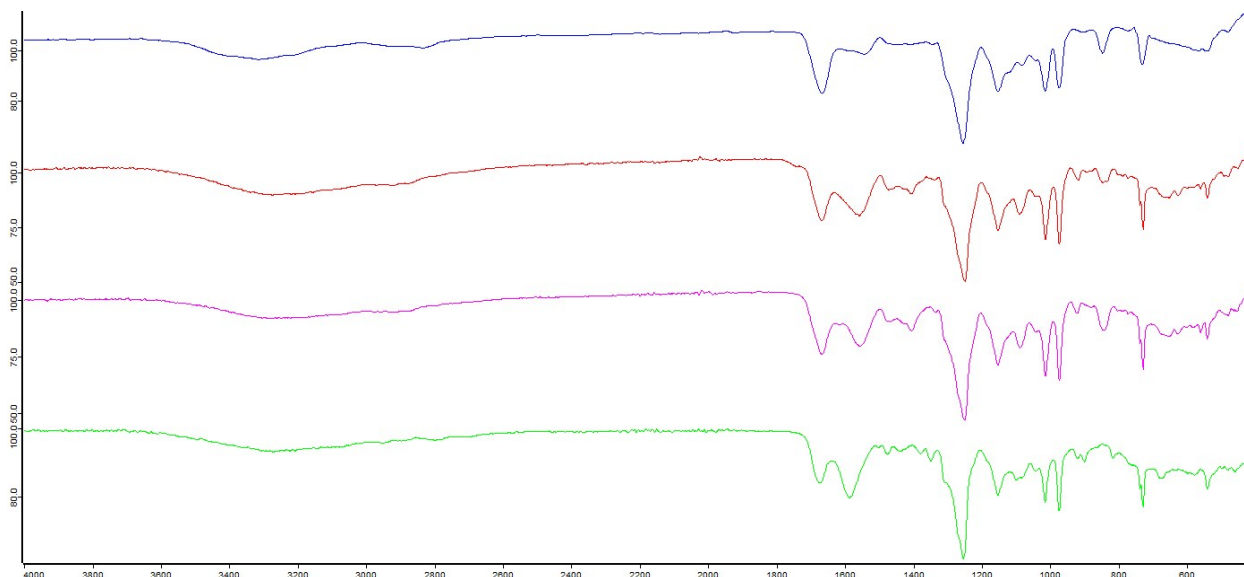


Figure S2. (Top to bottom) IR spectra of **L**, **FeL**, **CoL**, and **NiL**. The solid-state IR spectrum of **L** has a medium strong band at 1669 cm^{-1} due to the C=O stretch of the amide bond. The complexes display additional absorption bands at 1564 , 1558 , 1589 cm^{-1} , respectively, belonging to the metal coordinated carbonyl stretches.

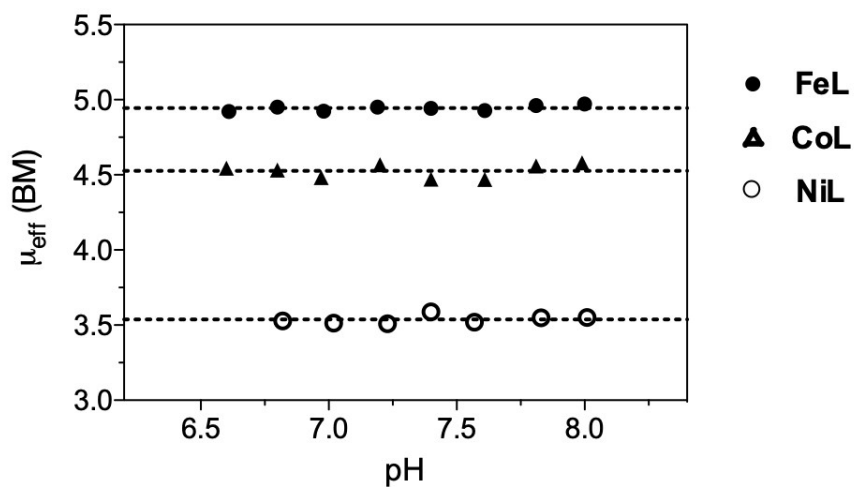


Figure S3. Measured effective magnetic moments of **FeL**, **CoL**, and **NiL** at different pH using Evans' Method. Dashed black line denotes the average value of μ_{eff} determined to be 4.94, 4.53, 3.54 BM.

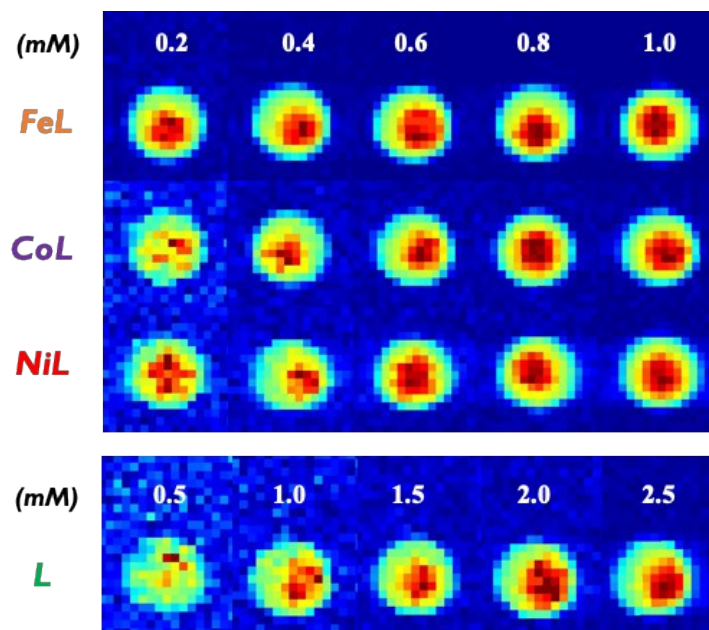


Figure S4. ^{19}F MR images of FeL, CoL, NiL, and L at different concentrations in 50 mM HEPES buffer (0.1 M NaCl, pH 7.4).

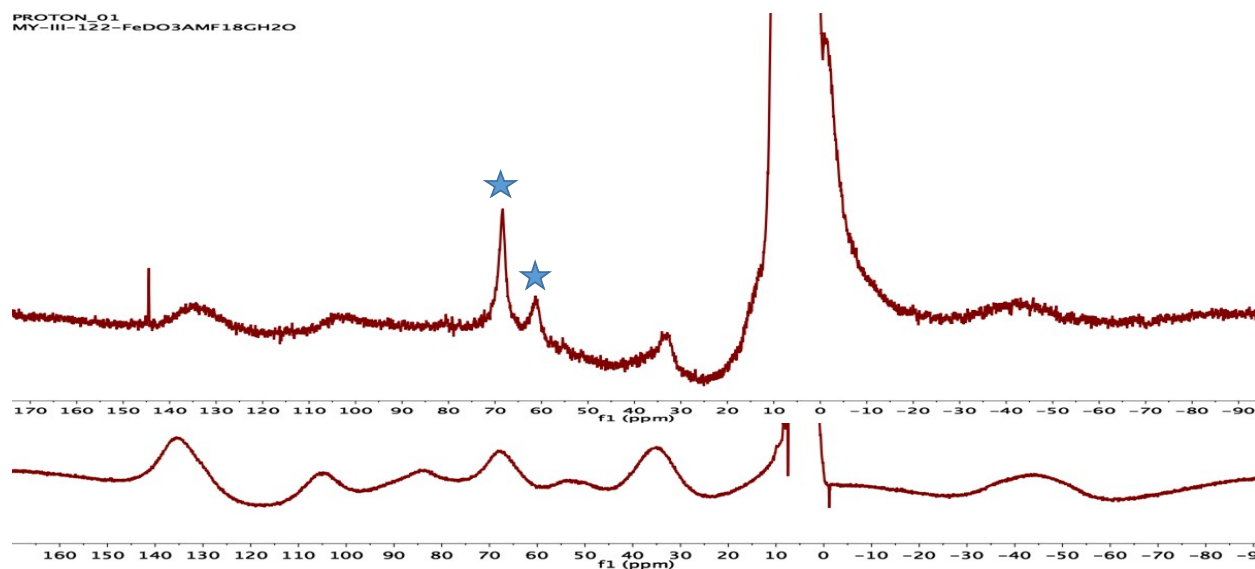


Figure S5. ^1H NMR spectra of FeL in HEPES buffer solutions (pH=7.4) of H_2O (top) and D_2O (bottom) at 23 °C. Stars at 68 and 62 ppm denote water exchangeable protons belonging to amide protons. Peak at 145 ppm (top) is a result of instrumental artifact.

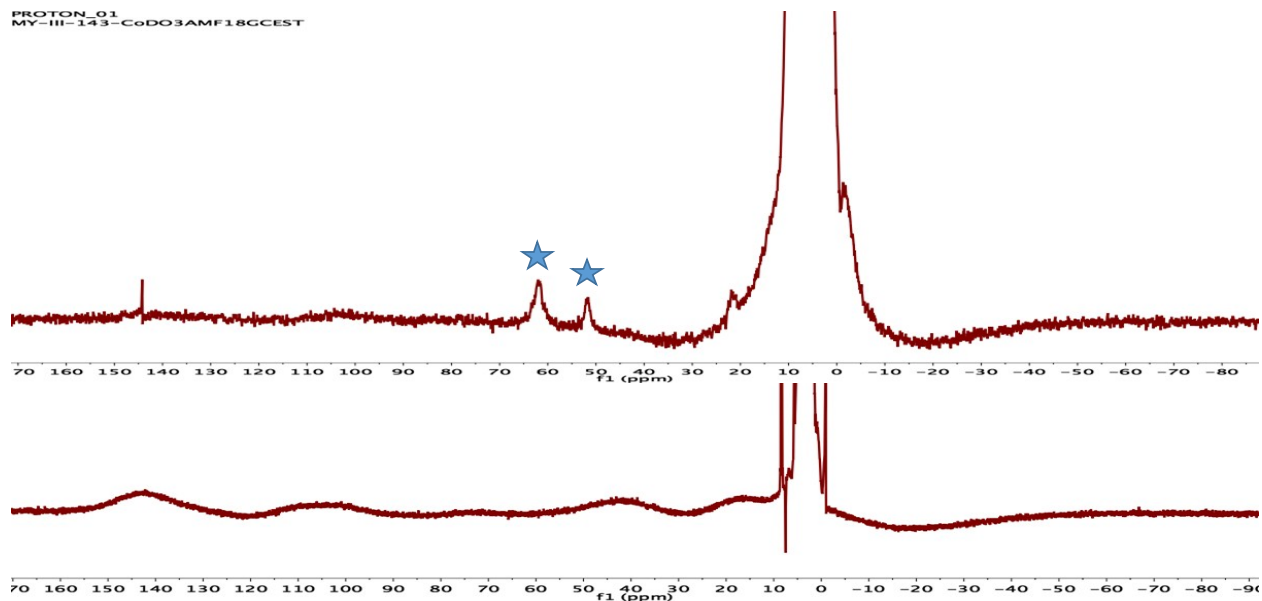


Figure S6. ^1H NMR spectra of **CoL** in HEPES buffer solutions (pH=7.4) of H_2O (top) and D_2O (bottom) at 23 °C. Stars at 62 and 52 ppm denote water exchangeable protons belonging to amide protons. Peak at 145 ppm (top) is a result of instrumental artifact.

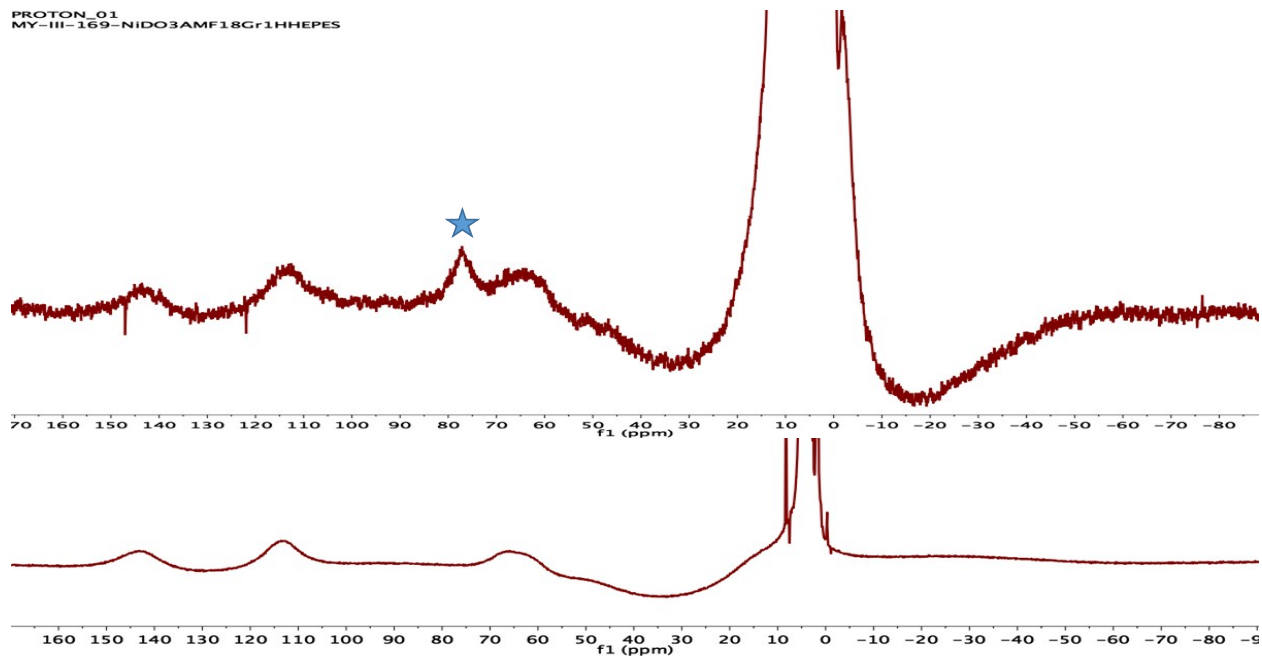


Figure S7. ^1H NMR spectra of **NiL** in HEPES buffer solutions (pH=7.4) of H_2O (top) and D_2O (bottom) at 23 °C. Star at 77 ppm denotes water exchangeable protons belonging to amide protons. Peaks at 147 ppm and 122 ppm (top) are due to instrumental artifact.

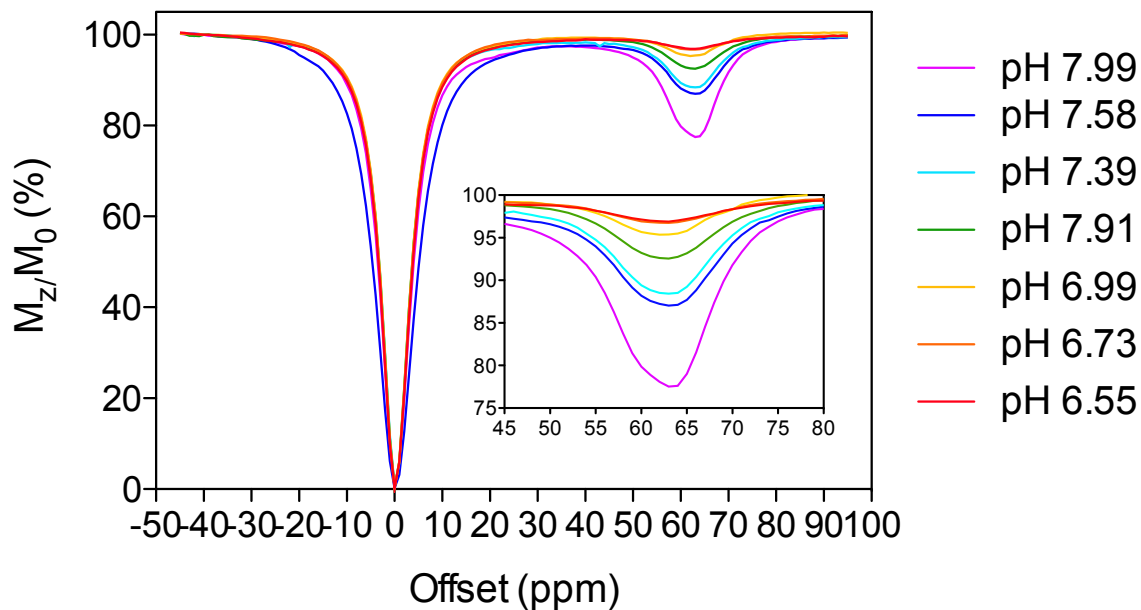


Figure S8. CEST spectra collected at 23 °C for 10.5 mM aqueous solutions of FeL in 50 mM HEPES and 100 mM NaCl buffered at pH 6.50-8.06 with a 4 s saturation pulse at $B_1 = 25 \mu\text{T}$.

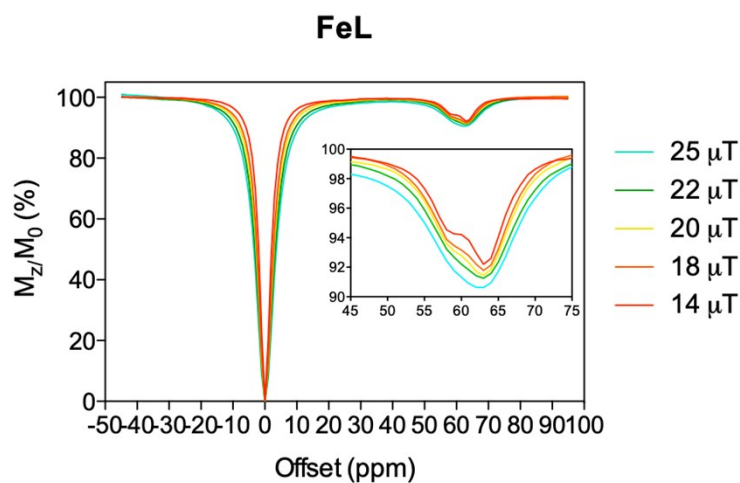


Figure S9. CEST spectra collected at 23 °C for 8.5 mM aqueous solutions of FeL in 50 mM HEPES and 100 mM NaCl buffered at pH 7.32 with a 4 s saturation pulse at power level (B_1) from 14.0 μT to 25.0 μT . Note that a secondary CEST feature emerges around 59 ppm at lower power level.

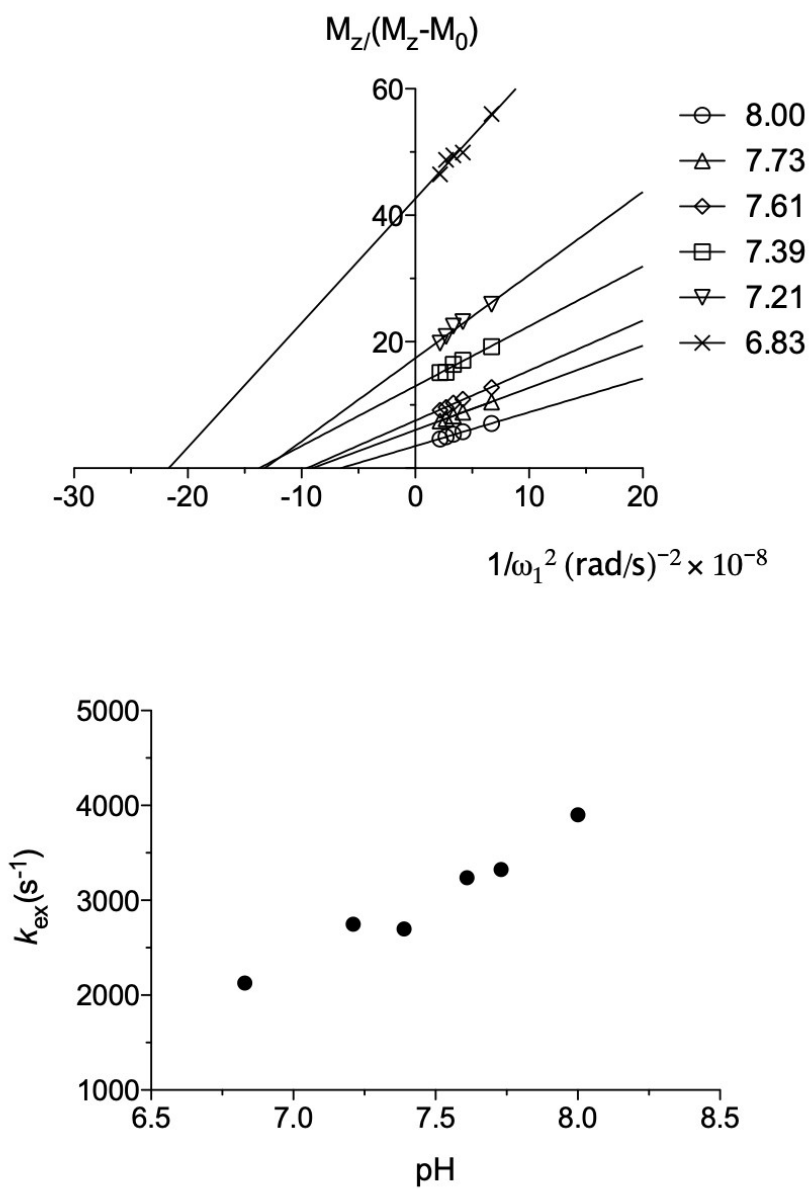


Figure S10. (Top) Omega plots of FeL from application of 4 s presaturation at 63 ppm using $B_1=14.0$ – 25.0 μ T for 9 mM of FeL in aqueous solutions containing 50 mM HEPES and 100 mM NaCl buffered to pH 6.83–8.0 collected at 23 °C and 9.4 T. (Bottom) Calculated k_{ex} using Omega plot versus pH. Note that the exchange rate gradually increases with pH.

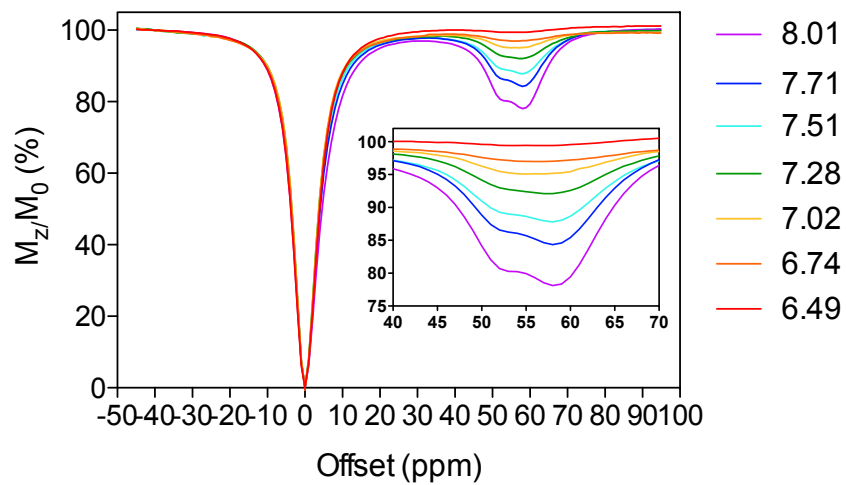


Figure S11. CEST spectra collected at 23 °C for 10.9 mM aqueous solutions of CoL in 50 mM HEPES and 100 mM NaCl buffered at pH 6.49-8.01. Power level $B_1 = 25.0 \mu\text{T}$, 4 s saturation pulse.

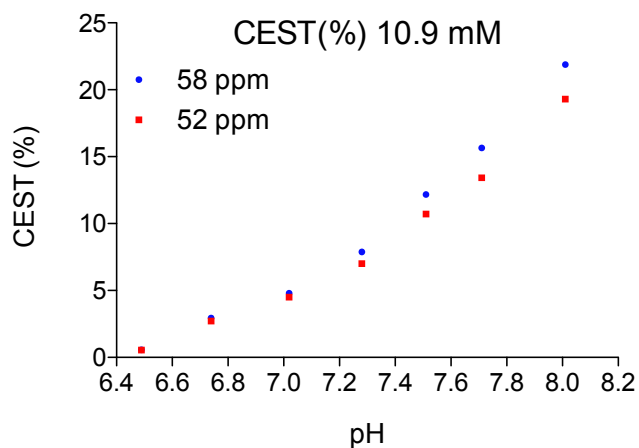


Figure S12. CEST intensity at 58 ppm and 52 ppm collected at 23 °C for 10.9 mM aqueous solutions of CoL in 50 mM HEPES and 100 mM NaCl buffered at pH 6.49-8.01. Power level $B_1 = 25.0 \mu\text{T}$, 4 s saturation pulse.

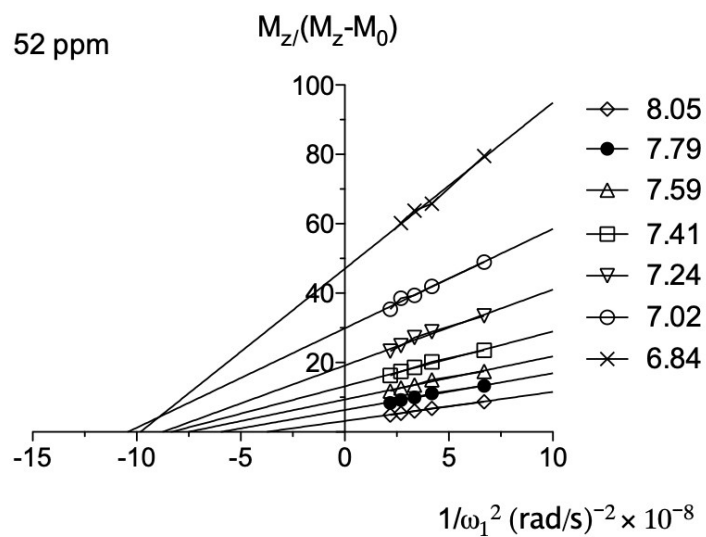
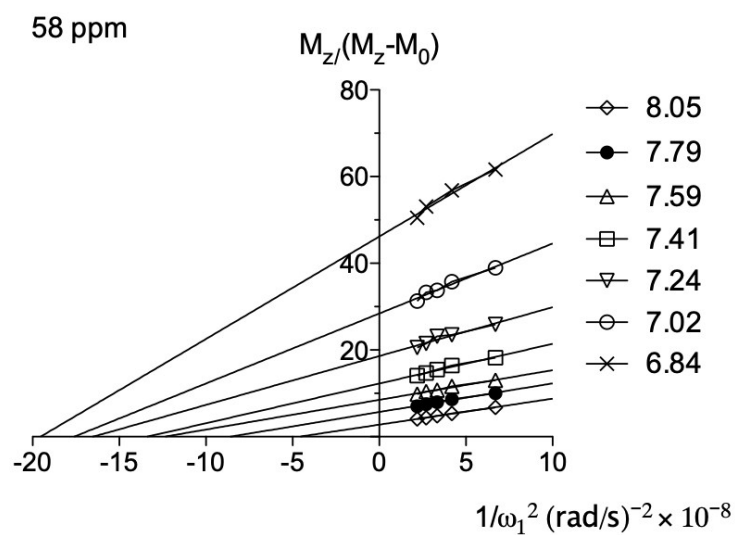


Figure S13. Omega plots of **CoL** from application of 4 s presaturation at 58 and 52 ppm using $B_1=14.0\text{--}25.0 \mu\text{T}$ for 10.0 mM of **CoL** in aqueous solutions containing 50 mM HEPES and 100 mM NaCl buffered to pH 6.84–8.05 collected at 23 °C and 9.4 T.

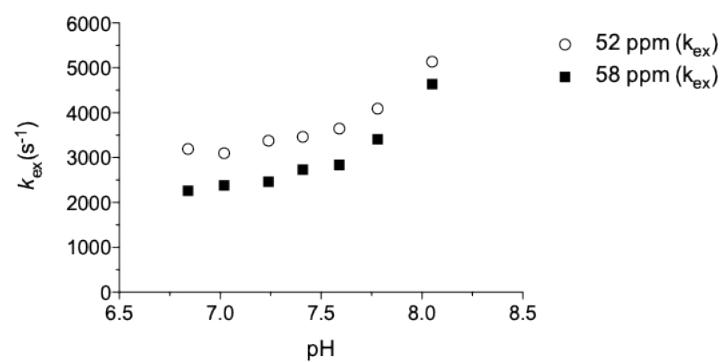


Figure S14. Calculated k_{ex} values at 58 ppm and 52 ppm for **CoL** using Omega plot versus pH. Note that the proton exchange rate at 52 ppm is faster than 58 ppm.

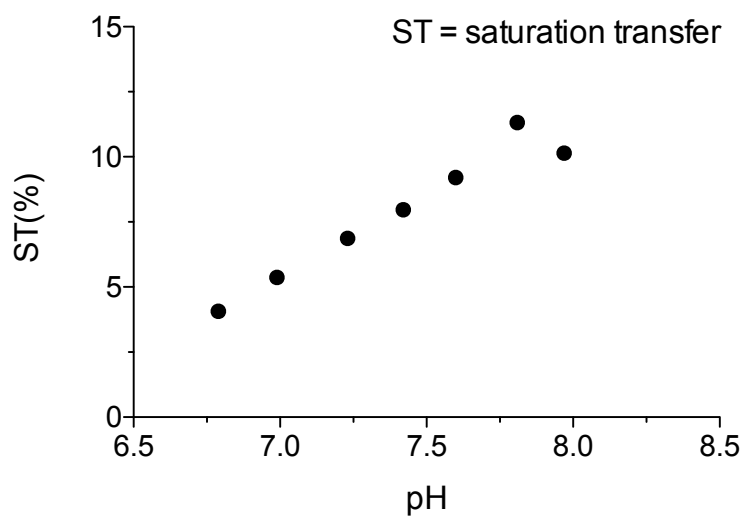
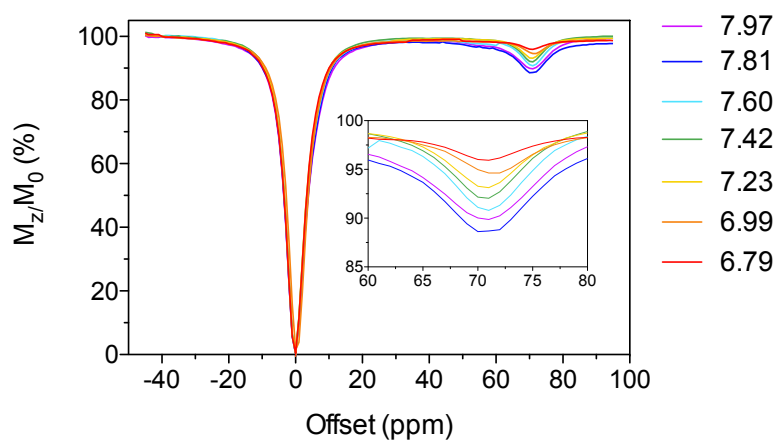


Figure S15. (Top) CEST spectra collected at 23 °C for 8.9 mM aqueous solutions of NiL in 50 mM HEPES and 100 mM NaCl buffered at pH 6.79-7.97. Power level $B_1 = 25.0 \mu\text{T}$, 4 s saturation pulse. (Bottom) Saturation transfer (ST) percentage vs pH. Note the ST reaches a plateau around pH=7.8.

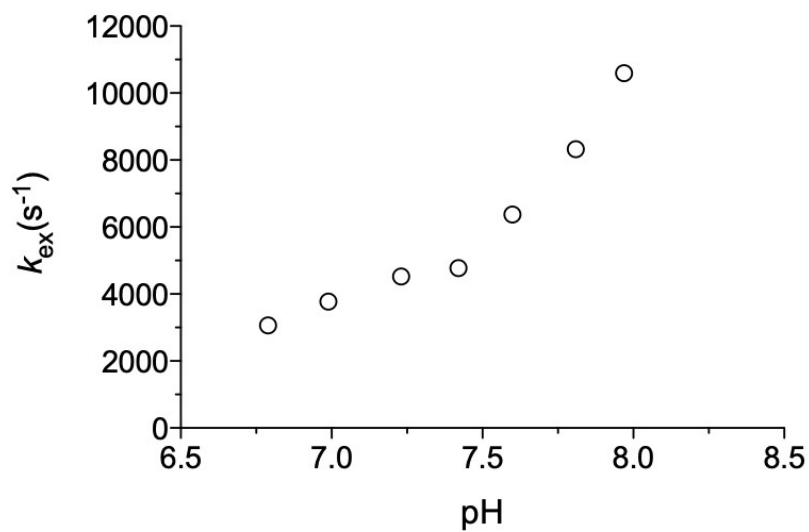
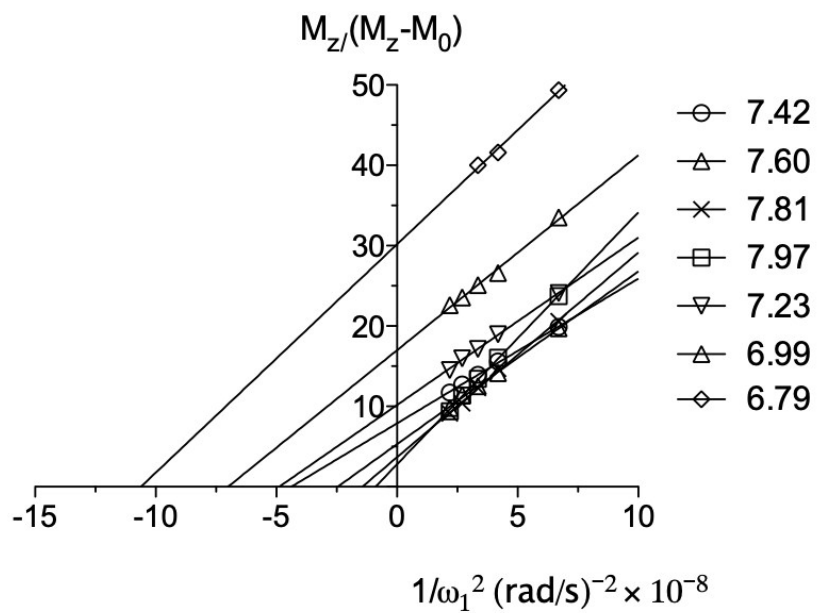


Figure S16. (Top) Omega plots of NiL from application of 4 s presaturation at 73 ppm using $B_1=14.0\text{--}25.0 \mu\text{T}$ for 9.0 mM of NiL in aqueous solutions containing 50 mM HEPES and 100 mM NaCl buffered to pH 6.79–7.94 collected at 23 °C and 9.4 T. (Bottom) Calculated k_{ex} using Omega plot versus pH. Note that the exchange rate gradually increases with pH.

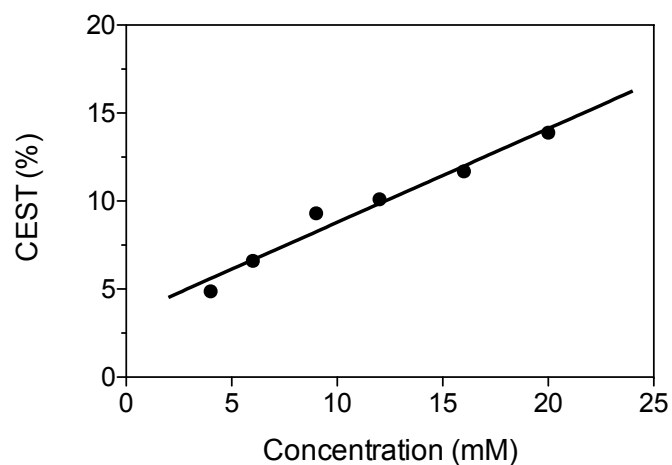
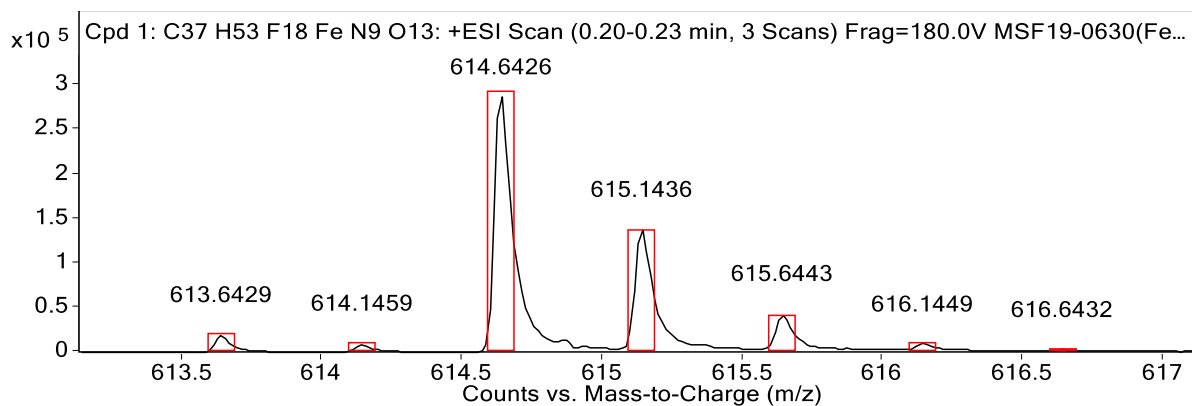


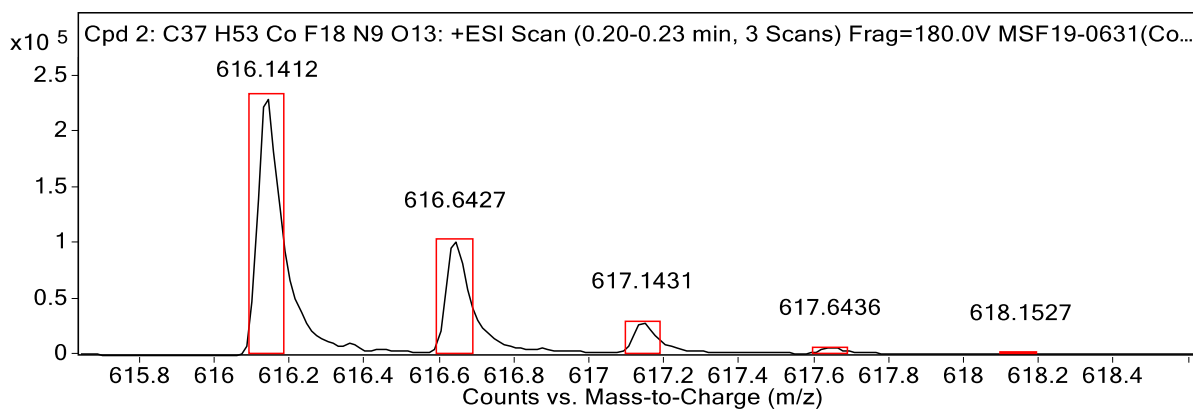
Figure S17. CEST% of FeL solution at variable concentration, pH 7.4, $B_1=25.0 \mu\text{T}$.



MS Spectrum Peak List

Obs. m/z	Calc. m/z	Charge	Abundance	Formula	Ion Species	Tgt Mass Error (ppm)
613.6429	613.6430	2	18173	C37H53F18FeN9O13	M+2	0.14
614.1459	614.1445	2	8544	C37H53F18FeN9O13	M+2	-2.28
614.6426	614.6407	2	288349	C37H53F18FeN9O13	M+2	-3.12
615.1436	615.1421	2	136719	C37H53F18FeN9O13	M+2	-2.47
615.6443	615.6433	2	41992	C37H53F18FeN9O13	M+2	-1.68
616.1449	616.1445	2	7544	C37H53F18FeN9O13	M+2	-0.67
616.6432	616.6456	2	1336	C37H53F18FeN9O13	M+2	3.82
617.1404	617.1467	2	525	C37H53F18FeN9O13	M+2	10.16
617.6569	617.6478	2	227	C37H53F18FeN9O13	M+2	-14.76

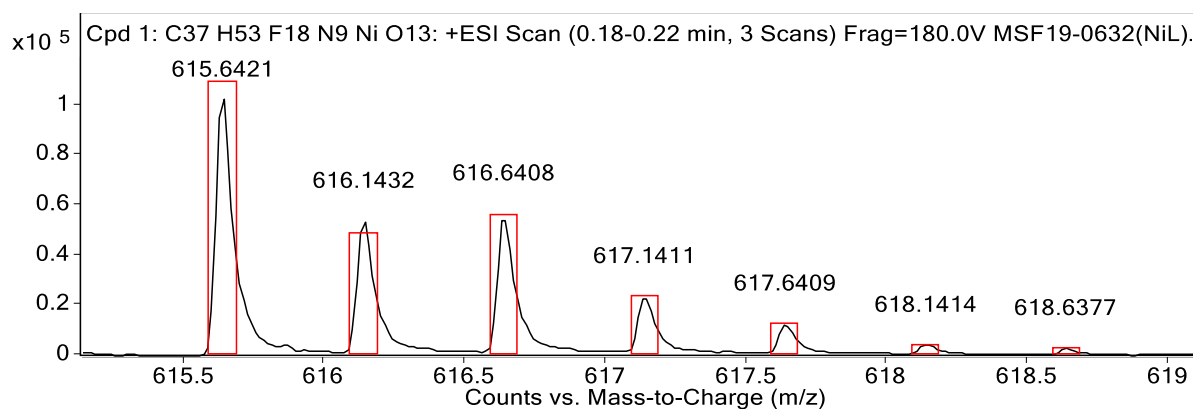
Figure S18. High resolution mass spectrum of FeL.



MS Spectrum Peak List

Obs. m/z	Calc. m/z	Charge	Abundance	Formula	Ion Species	Tgt Mass Error (ppm)
616.1412	616.1398	2	233349	C37H53CoF18N9O13	M+2	-2.24
616.6427	616.6413	2	102243	C37H53CoF18N9O13	M+2	-2.27
617.1431	617.1426	2	29588	C37H53CoF18N9O13	M+2	-0.87
617.6436	617.6438	2	5759	C37H53CoF18N9O13	M+2	0.36
618.1527	618.1451	2	934	C37H53CoF18N9O13	M+2	-12.42
618.6313	618.6463	2	457	C37H53CoF18N9O13	M+2	24.27

Figure S19. High resolution mass spectrum of CoL.



MS Spectrum Peak List

Obs. m/z	Calc. m/z	Charge	Abundance	Formula	Ion Species	Tgt Mass Error (ppm)
615.6421	615.6409	2	103232	C37H53F18N9NiO13	M+2	-1.95
616.1432	616.1424	2	53515	C37H53F18N9NiO13	M+2	-1.41
616.6408	616.6398	2	56533	C37H53F18N9NiO13	M+2	-1.54
617.1411	617.1406	2	23397	C37H53F18N9NiO13	M+2	-0.82
617.6409	617.6396	2	12429	C37H53F18N9NiO13	M+2	-2.12
618.1414	618.1402	2	3853	C37H53F18N9NiO13	M+2	-2.02
618.6377	618.6387	2	2582	C37H53F18N9NiO13	M+2	1.6

Figure S20. High resolution mass spectrum of NiL.

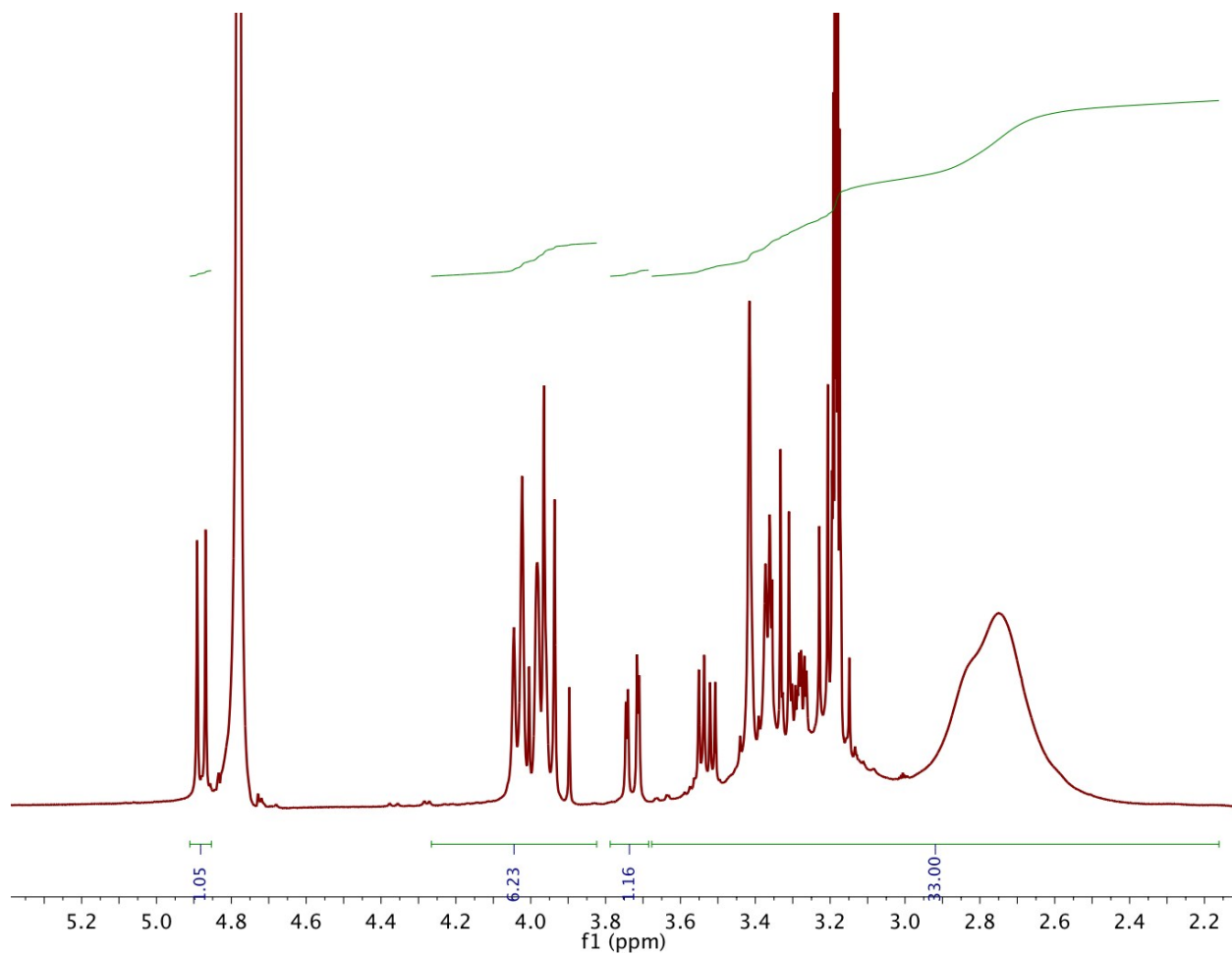


Figure S21. ^1H NMR spectrum of **L** in CD_3OD .

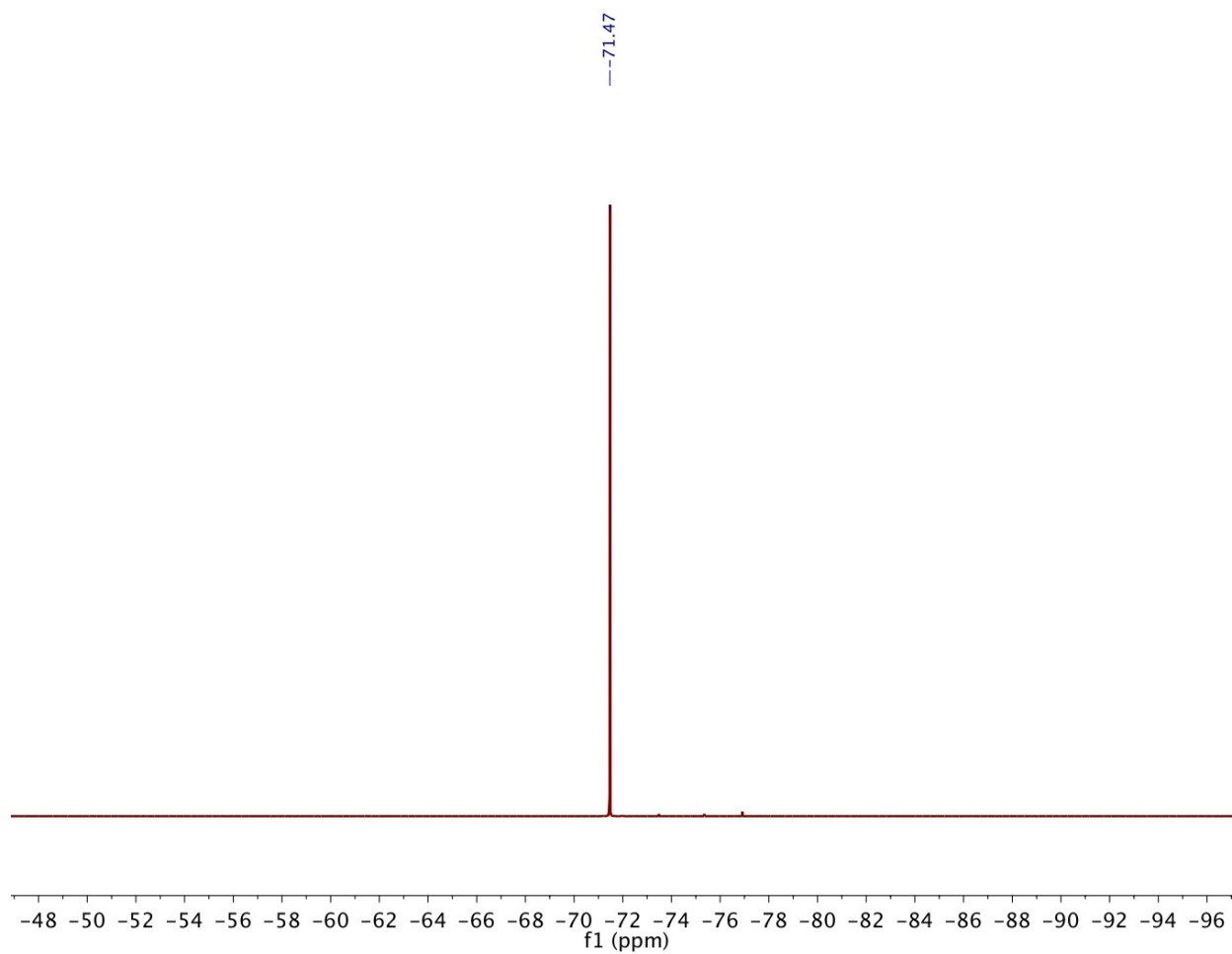


Figure S22. ^{19}F NMR spectrum of **L** in CD_3OD .

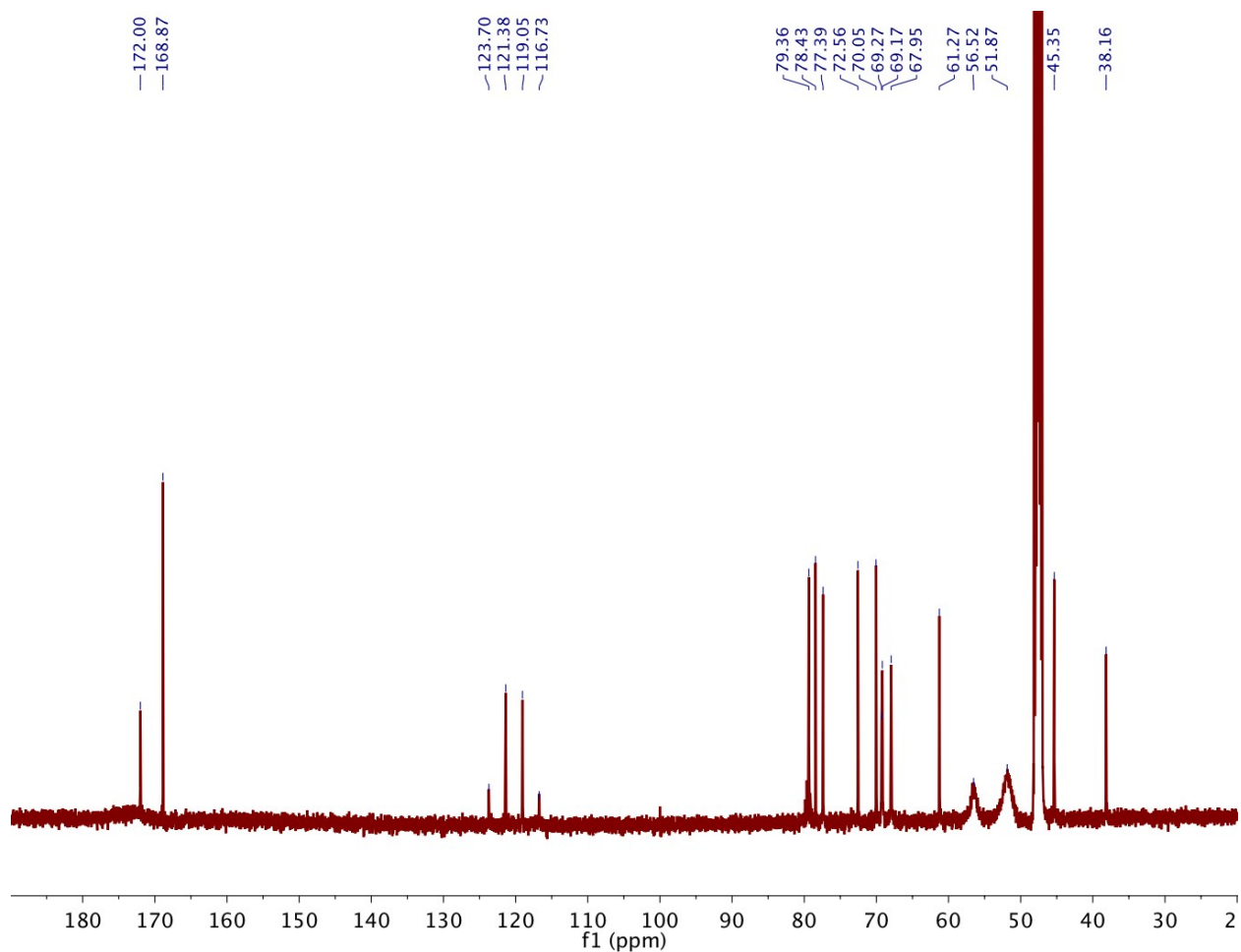


Figure S23. ^{13}C NMR spectrum of **L** in CD_3OD .

References

- 1 S. Kawasaki, T. Muraoka, T. Hamada, K. Shigyou, F. Nagatsugi and K. Kinbara, *Chemistry – An Asian Journal*, 2016, **11**, 1028–1035.
- 2 Y. Tang, S. Zhang, Y. Chang, D. Fan, A. De Agostini, L. Zhang and T. Jiang, *J. Med. Chem.*, 2018, **61**, 2937–2948.
- 3 H. Akiba, J. Sumaoka, K. Tsumoto and M. Komiyama, *Anal. Chem.*, 2015, **87**, 3834–3840.
- 4 D. F. Evans, *J. Chem. Soc.*, 1959, 2003.
- 5 G. A. Bain and J. F. Berry, *J. Chem. Educ.*, 2008, **85**, 532.